Tuning the range of spatial coupling in electrochemical systems: From local via nonlocal to global coupling

Nadia Mazouz, Georg Flätgen,* and Katharina Krischer†
Fritz-Haber-Institut der Max-Planck-Gesellschaft, Faradayweg 4-6, D-14195 Berlin (Dahlem), Germany
(Received 01 October 1996)

A specific feature of pattern formation in electrochemical systems is the occurrence of accelerated fronts; they can be attributed to long-range spatial coupling. In this paper we demonstrate that different coupling functions can be realized by tuning easily accessible parameters: The range of the coupling crucially depends on the length scales of the system, and the strength of the coupling is proportional to the conductivity of the electrolyte. Simulations in the bistable regime are presented which illustrate how the front behavior changes qualitatively when length scales or conductivity are varied. [S1063-651X(97)12702-7]

PACS number(s): 64.10.+h, 82.20.Mj, 82.45.+z, 47.54.+r

INTRODUCTION

Reaction-diffusion equations proved to be well suited for describing many different dynamical regimes of dissipative systems [1,2]. An implicit assumption when modeling spatial communication by a diffusional process is that only nearest neighbors communicate with each other, or, in other words, that the spatial coupling is local or short range. Evidently this prerequisite does not always hold, and recently the impact of global coupling on pattern formation has become an active area of research.

In a globally coupled system a change of state of the system at a certain location is felt equally by all other parts of the system. Examples where global coupling turned out to be essential for the description of the spatiotemporal dynamics are CO oxidation at Pt single-crystal surfaces [3–6] as well as at supported catalysts [7], semiconductor devices with a load resistor in series [8–10], or gas discharge tubes [11–13]. The influence of a global feedback on the dynamics of spiral waves was demonstrated with the light-sensitive Belousov-Zhabotinsky reaction [14]. The important role global coupling can play for spatiotemporal dynamics was confirmed in theoretical studies, which proved the influence of the global coupling in a particular system or generally classified patterns that can arise in a certain dynamic regime if global coupling is added [15–22].

Besides these two extreme cases, local coupling, on the one hand, and global coupling, on the other hand, any variation in range and strength of coupling is possible. In fact nonlocal coupling, defined by a characteristic distance over which the state of the system at one point influences other parts of the system with a distance-dependent strength, can be viewed as the general case. From this point of view, local and global coupling are the two limits of nonlocal coupling, with the range going to zero and infinity, respectively. Moreover, long-range coupling is always to be expected when the spatial coupling occurs via electric fields. This kind of transport mechanism is important in a variety of systems, among them, e.g., synaptic coupling of neurons.

There are comparatively few investigations of spatiotemporal dynamics of systems with nonlocal coupling. For example, Schimanski-Geier, Zülicke, and Schöll described the growth of domains in the bistable regime in the presence of nonlocal interactions [23]. Elmer considered spatially extended systems with nonlocal dynamics near the soft mode instability of a stable and uniform state [24]. Kuramoto derived the complex Ginzburg-Landau equation for nonlocal coupling in a general form, and obtained some astonishing results on the scaling behavior of turbulent oscillators [25–27]. Recently it has been shown that spatial coupling in electrochemical systems occurs via migration currents in the electrolyte, and is intrinsically nonlocal [28,29]. In these systems an accelerated motion of interfaces was observed in the bistable, excitable, and oscillatory regimes [28,30–32], which was attributed to the nonlocal coupling [28,29].

In this paper, we discuss various aspects of the nonlocal coupling in electrochemical systems. In particular we show that the range of the coupling can be varied continuously, and we discuss the effect of the range of the coupling on the dynamic behavior in the bistable regime. As electrochemical systems have many similarities with other systems that serve as models for the study of pattern formation, e.g., semiconductor and other electronic devices or gas discharge tubes, results presented here give a guideline of how to establish or avoid long-range coupling experimentally, and how to adjust its range. In Sec. II we give a short review of the properties of electrochemical systems which are important in our context and how they are modeled. A detailed derivation and discussion of the model can be found in [29,33]. In Sec. III the nature of the long-range coupling and its parameter dependence are elaborated and substantiated by simulations. Finally, we discuss in which range the coupling can be tuned as well as the connection of the model considered here with another model for electrochemical systems which is of the reaction-diffusion type [34].

SYSTEM AND MODEL

Electrochemical reactions take place at the electrode-electrolyte interface, the reaction rate being decisively deter-

*Present address: Department of Chemical Engineering, University of Princeton, Princeton, NJ 08544.
†Author to whom correspondence should be addressed. Electronic address: krischer@fhi-berlin.mpg.de

 © 1997 The American Physical Society

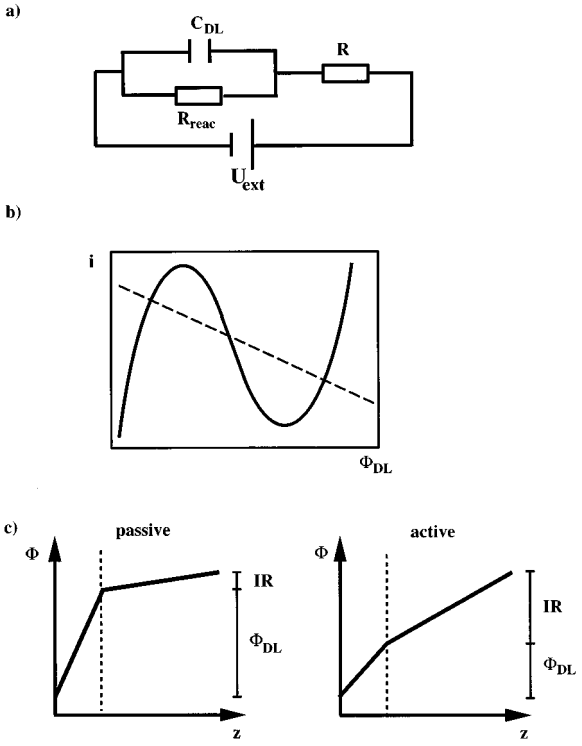

FIG. 1. (a) Equivalent circuit of an electrochemical cell. (b) N-shaped current-potential characteristic of i_{reac} (solid line) and load line (dashed curve). (c) Schematics of the potential across the cell for the two steady states in the bistable regime.

mined by the potential drop across the interface, the so-called double layer. In an electrochemical experiment this potential drop, and thus the reaction rate, is usually controlled with a potentiostat, i.e., an electronic device that keeps constant the potential difference between the working electrode and an auxiliary or reference electrode. In the simplest approximation, the electrical properties of an electrochemical cell can be described by the equivalent circuit shown in Fig. 1(a). Here the electrode-electrolyte interface is viewed as a parallel connection of a capacitor and a non-Ohmic resistor that possesses the current-voltage characteristic of the respective reaction. The Ohmic resistor in series with the interface circuit represents the electrolyte between working and reference electrode, and a constant voltage U_{ext} is applied between these two electrodes. This voltage is an important control parameter in electrochemical systems, and it is obviously composed of the potential drop across the double layer ϕ_{DL} and the potential drop in the electrolyte IR, where I is the total current flowing through the cell and R the electrolyte resistance. Hence the potentiostatic operation mode leads to the constraint $U_{\mathrm{ext}}=\phi_{\mathrm{DL}}+IR$, and the equation governing the circuit is given by

$$C_{\mathrm{DL}}\frac{d\phi_{\mathrm{DL}}}{dt}=-i_{\mathrm{reac}}(\phi_{\mathrm{DL}})+\frac{U_{\mathrm{ext}}-\phi_{\mathrm{DL}}}{R}, \qquad (1)$$

where i_{reac} is the (negative) reaction current density, and C_{DL} the specific capacitance of the double layer. The second term is often referred to as the load line. It is interesting to note that the same equivalent circuit also arises in semiconductor physics, where the parallel connection of the capacitance and

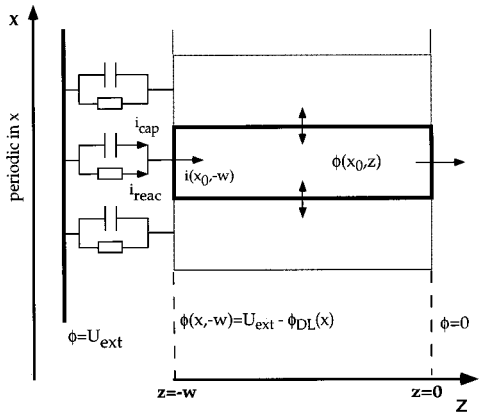

FIG. 2. Equivalent circuit for a spatially extended system. x: direction parallel to the electrode. z: direction perpendicular to the electrode.

nonlinear resistor symbolizes the semiconductor, and the Ohmic resistor represents an external load [8,35].

The stability of the circuit with different characteristics of the nonlinear resistance was studied extensively in the past [36–38]. In electrochemical systems, current-potential curves that play a role in a large class of reactions exhibiting dynamic instabilities possess an N-shaped characteristic as shown in Fig. 1(b). Obviously, the steady states of the equivalent circuit are intersections of the current-potential characteristics (i_{reac} vs ϕ_{DL}) and the load line. Bistable behavior can occur if the electrolyte resistance R is large enough, i.e., if $R>|d\phi_{\mathrm{DL}}/dI|$. The so called passive stable steady state is characterized by a large potential drop across the double layer which leads to a small current, and hence a small IR drop in the electrolyte. The active steady state possesses a small potential drop across the double layer causing a high current and hence a large IR drop [Fig. 1(c)].

To fully describe the electrochemical reaction along with the potential distribution, the concentrations of the reacting species have to be considered, and in addition to bistability, temporally periodic or chaotic behavior can occur [39]. However if the mass transport is efficient, i.e., if it is much faster than the reaction rate, changes of the concentrations can be neglected. In this case the concentration in front of the double layer becomes a parameter, and the potential is the only variable in the system. Experimentally, this situation can be realized with rotating electrodes [40]. In the following, we restrict our considerations to such conditions.

We are interested in spatial patterns that form in an electrochemical cell, and hence the picture has to be expanded by the spatial dimensions. Let us consider the simplest case: a one-dimensional electrode with periodic boundary conditions, an idealized description of a ring electrode whose diameter is large compared to the thickness of the ring. Figure 2 displays the corresponding equivalent circuit. Now, the electrode is viewed as being composed of an infinite number of infinitesimally small interface circuits which couple to the electrolyte, i.e., an electroneutral medium with the specific conductivity σ, and the whole circuit is described by the following equations for the potential in the electrolyte ϕ [29]:

$$\Delta\phi = 0, \tag{2a}$$

$$C_{\mathrm{DL}} \left.\frac{\partial \phi}{\partial t}\right|_{z=-w} = i_{\mathrm{reac}}(\phi_{\mathrm{DL}}) + \sigma \left.\frac{\partial \phi}{\partial z}\right|_{z=0} + \sigma \int_{-w}^{0} \frac{\partial^2 \phi}{\partial x^2}\, dz$$

$$\overset{(2a)}{=} i_{\mathrm{reac}}(\phi_{\mathrm{DL}}) + \sigma \left.\frac{\partial \phi}{\partial z}\right|_{z=-w}, \tag{2b}$$

$$\phi(x+L,z,t) = \phi(x,z,t), \tag{2c}$$

$$U_{\mathrm{ext}} = \phi_{\mathrm{DL}} + \phi(z=-w), \tag{2d}$$

$$\phi(x,z=0,t) = 0. \tag{2e}$$

Equation (2a) describes the potential distribution inside the electrolyte, which is due to the electroneutrality of the electrolyte given by Laplace's equation. Equations (2b)–(2e) are the corresponding boundary conditions, Eq. (2c) describing periodic boundary conditions parallel to the electrode where L is the length of the electrode. Equations (2d) and (2e) take into account the potentiostatic operation mode and the equipotential plane at the location of the reference electrode, i.e., at $z=0$, where the potential is arbitrarily set to zero. Equation (2b) describes the temporal evolution of the potential drop across the double layer, and results from a current balance through the boundaries of the area element $dx \cdot w$, where w is the distance between working and reference electrode. The three terms on the right hand side correspond to the reaction current density and the migration current densities perpendicular and parallel to the electrode, respectively. Their sum equals the capacitive charging of the interface at the location x_0. This time-dependent boundary condition is the source of any dynamic structure, or, in other words, patterns are generated at the electrode-electrolyte interface.

Using the dimensionless quantities,

$$\phi' = \frac{nF}{RT}\phi, \quad V = \frac{nF}{RT} U_{\mathrm{ext}}, \quad \phi'_{\mathrm{DL}} \frac{nF}{RT}\phi_{\mathrm{DL}},$$
$$t' = \frac{n^2F^2k_0c^b}{C_{\mathrm{DL}}RT}, \quad x' = \frac{2\pi}{L}x, \quad z' = \frac{1}{w}z \tag{3a}$$

with

$$x' \in [0,2\pi], \quad z' \in [-1,0], \tag{3b}$$

$$\sigma' = \frac{1}{RTk_0c^b}\frac{\sigma}{L}, \quad i'_{\mathrm{reac}} = \frac{1}{nFk_0c^b} i_{\mathrm{reac}}, \tag{4}$$

where F is Faraday's constant, n the charge number, k_0 the reaction rate, c^b the bulk concentration of the reacting species, R the gas constant, and T the absolute temperature, Eq. (2b) becomes (the primes have been omitted for clarity)

$$\left.\frac{\partial \phi}{\partial t}\right|_{z=-1} = i_{\mathrm{reac}}(\phi) + \sigma \frac{L}{w} \left.\frac{\partial \phi}{\partial z}\right|_{z=-1}. \tag{5}$$

Note that the specific conductivity σ in Eq. (2b) enters only (and linearly) in the parameter σ' in Eq. (5). In order to emphasize the importance of the conductivity for the behavior of the system, we also refer to the parameter σ as specific conductivity throughout the text. The dimensionless reaction current density was described by the following expression, which was adjusted for the special case of our experiment:

$$i_{\mathrm{reac}}(\phi_{\mathrm{DL}}) = (0.0365\phi_{\mathrm{DL}}^3 + 17.23\phi_{\mathrm{DL}}^2 + 2039.6\phi_{\mathrm{DL}}). \tag{6}$$

Using Eq. (2d) this ϕ_{DL}-dependent expression can be expressed as a polynome in ϕ, with coefficients that are functions of the dimensionless externally applied voltage V.

With given initial conditions for the potential at the electrode and the boundary conditions (2c)–(2e), the solution of Laplace's equation is given by the following series:

$$\phi(x,z,t) = \sum_{n=1}^{\infty} (\tilde{A}_n(z,t)\cos[nx] + \tilde{B}_n(z,t)\sin[nx]) + \tilde{A}_0(z,t), \tag{7a}$$

with z and time-dependent coefficients:

$$\tilde{A}_n(z,t) = \sinh\left[\frac{w}{L} 2\pi n z\right] a_n(t), \tag{7b}$$

$$\tilde{B}_n(z,t) = \sinh\left[\frac{w}{L} 2\pi n z\right] b_n(t), \tag{7c}$$

$$\tilde{A}_0(z,t) = z a_0(t), \tag{7d}$$

Hence the Fourier functions are the natural basis functions of our problem, and it is advantageous to project Eq. (5) onto this basis. Substituting Eqs. (7a)–(7d) into Eq. (5) leads to an infinite number of ordinary differential equations for the coefficients $A_i(t) = -\tilde{A}_i\ (z=-1,\ t)$ and $B_i(t) = -\tilde{B}_i\ (z=-1,\ t)$ of the Fourier series at $z=-1$, i.e., at the electrode:

$$\frac{dA_0}{dt} = -f_0(A_1, B_i) - \frac{\sigma L}{w} A_0, \tag{8a}$$

$$\frac{dA_n}{dt} = -f_n(A_i, B_i) - \sigma\, 2\pi n\, \coth\left(\frac{w}{L} 2\pi n\right) A_n, \tag{8b}$$

$$\frac{dB_n}{dt} = -f_n(A_i, B_i) - \sigma\, 2\pi n\, \coth\left(\frac{w}{L} 2\pi n\right) B_n, \tag{8c}$$

where the functions $f_n(A_i, B_i)$ represent the projection of the reaction current i_{reac} density onto the coefficient space.

In the numerical simulations Eqs. (8a)–(8c) were integrated with the livermore solver for ordinary differential equations (lsode) [41], using 2×150 nontrivial cosine and sine modes. The functions f_n were evaluated in physical space, whereby $3\times2\times150$ collocation points were used for the fast Fourier transform back into the coefficient space [42].

RESULTS

In order to understand the spatial coupling through the electrolyte, we have to analyze the potential distribution and its impact on the dynamics as a function of the parameters. First, consider Eqs. (7a)–(7d), which describe the potential distribution in the electrolyte. In the direction perpendicular to the electrode (the z direction) the coefficients in the Fourier series are damped proportionally to $\sinh[(w/L)2\pi nz]$ which means that short wavelengths are damped more rapidly into the electrolyte than large wavelengths, leading to the delocalization of a structure localized at the electrode. The way the modes are damped into the electrolyte also depends on the ratio of the two length scales of the system, the distance w between working electrode and equipotential line

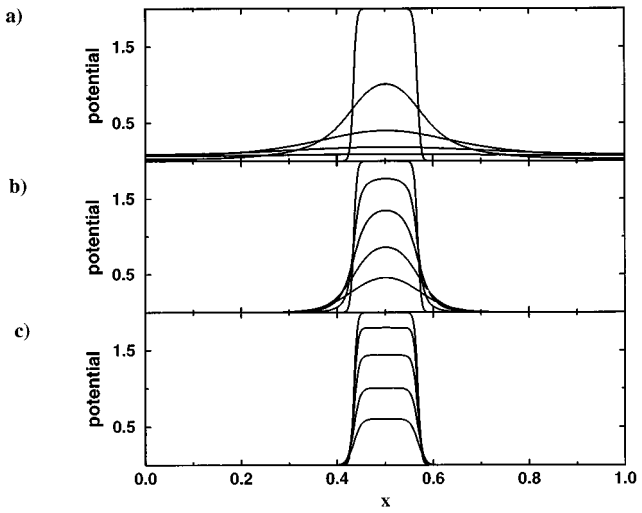

FIG. 3. Potential distribution as a function of x for five locations z_i in the electrolyte, and three values of w/L. (a) $2\pi w/L=4$. (b) $2\pi w/L=0.5$. (c) $2\pi w/L=0.1$. ($z_i=-1$, -0.9, -0.8, -0.7, and -0.6; note that $z_i=-1$ is at the electrode, i.e., the potential distribution chosen.)

and the circumference L of the electrode. This parameter significantly influences the effectiveness of the delocalization. In Fig. 3, cuts of the potential are shown at four equally spaced distances from the electrode for three different ratios of w/L, where w/L decreases from Fig. 3(a) to Fig. 3(c). Obviously, the delocalization of an inhomogeneity at the electrode is suppressed if the equipotential line is located very close to the electrode.

The amount of the delocalization of potential inhomogeneities at the electrode affects the temporal dynamics of the coefficients: Due to the interplay of Laplace's equation (2a) and the integral term in Eq. (2b) a perturbation at a location x_0 at the electrode is felt even at a position far away from x_0. This also becomes apparent in the second term of Eqs. (8b) and (8c), which represents this interplay, i.e., it gives the spatial coupling term in mode representation. In this form the different parameter dependence of the spatial coupling in reaction-diffusion systems and in electrochemical systems can be seen best. The former gives rise to a term proportional to $-n^2$, i.e., a parameter affects the damping of all modes equally. In contrast, the latter is proportional to $-2\pi n \coth((w/L)2\pi n)$ and hence *the ratio of the damping terms of different modes* changes when the geometric parameter w/L is varied. This allows us to adjust the range of the coupling: for large values w/L the coupling is long range, whereas for small values w/L it becomes short range or local.

Simulations of Eqs. (8a)–(8c) in the bistable regime for different ratios w/L are reproduced in Fig. 4. The initial conditions, equal in all four cases, were chosen such that a small portion of the electrode was set in the high-current steady state, and the remaining electrode in the low-current steady state. As a variation of w/L alone would alter the local dynamics and hence the steady states of the system, σ was adjusted such that the product $\sigma(L/w)$ remained constant. From the spatiotemporal picture (Fig. 4, top) as well as from the global current (Fig. 4 bottom), it is apparent that the spatiotemporal behavior is quite different in the four cases. For small w/L [Fig. 4(a)], the interface is sharp, and seems to propagate with constant velocity; the global current changes linearly. When increasing w/L [Figs. 4(b) and 4(c)] the interface becomes broader and, more remarkably, it does not move with a constant velocity but with an increasing velocity. This is typical for fronts [43] observed in the above-cited experiments. If the electrode becomes very short in comparison to its distance to the equipotential line, the initially inhomogeneous potential distribution disappears in a short transient after which the transition appears to occur homogeneously over the whole electrode [Fig. 4(d)].

Figure 4 suggests that w/L, and hence the range of the coupling, has a strong influence on the spatiotemporal behavior of electrochemical systems in the bistable regime. However, the interpretation of the simulations is not that straightforward as two parameters, σ and w/L, were varied so that the homogenous state remained the same. In a computer experiment the local dynamics can be easily decoupled from the spatial coupling term, and in this way it is possible to

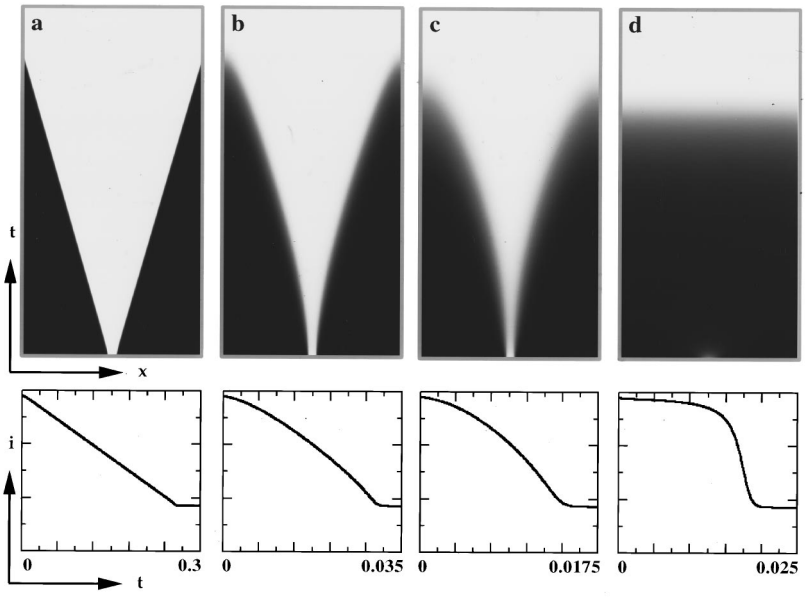

FIG. 4. Gray scale representation of the spatiotemporal evolution of the potential at $z=-1$ (above) and time series of the global current (below) in the bistable regimes for four values of w/L. (a) $w/L=0.0477$, $\sigma=0.477$; (b) $w/L=0.477$, $\sigma=4.77$; (c) $w/L=1.5957$, $\sigma=15.957$; (d) $w/L=15.957$, $\sigma=159.57$ (remaining parameter: $V=-350$)..

study the influence of range and strength of the coupling separately.

From the equivalent circuits in Figs. 1(a) and 2, as well as from Eqs. (1) and (2a)–(2e), it is evident that the homogeneous steady states, i.e., the local dynamics, are given by

$$\left.\frac{d\phi}{dt}\right|_{z=-1} = i_{\mathrm{reac}}(\phi) + \frac{\sigma L}{w}\,\phi\Big|_{z=-1}. \tag{9}$$

Hence the second terms in Eqs. (8b) and (8c) contain a part that belongs to the local dynamics, namely, $(-\sigma L/w)A_n$. The spatial coupling without the contribution to the local dynamics is obviously given by

$$\left[-\sigma\, 2\pi n\, \coth\left(\frac{w}{L} 2\pi n\right) + \frac{\sigma L}{w}\right] A_n .$$

Thus, when writing Eqs. (8b) and (8c) in the form

$$\frac{dA_n}{dt} = -f_n(A_i, B_i) - \frac{\sigma L}{w} A_n - \left[\tilde{\sigma}\, 2\pi n\, \coth\left(\frac{\tilde{w}}{L}\, 2\pi n\right) - \frac{\tilde{\sigma} L}{\tilde{w}}\right] A_n , \tag{10}$$

it is possible to separate the contribution of σ and (w/L) to the local dynamics from their contribution to the spatial coupling, and the effect of the parameters on range and strength can be studied separately by varying $\tilde{w}/L$ and $\tilde{\sigma}$, respectively.

First, let us look at the x dependence of the spatial coupling term. Figure 5(a) displays the spatial coupling term for a rectangular (though differentiable in C^n) perturbation of the potential at the electrode for different values of $\tilde{w}/L$, the coupling strength $\tilde{\sigma}$ being set to 1. Although the potential distribution possesses two sharp interfaces, their influence is felt at every point for large values of $\tilde{w}/L$, though with decreasing intensity for increasing distance, as is typical of nonlocal or long-range coupling. The range of the coupling decreases with $\tilde{w}/L$ until the interface affects only its nearest neighbors. Hence in this case the coupling is short range or local, as it is also characteristic of diffusional coupling. For comparison, the diffusional coupling with the same initial conditions is shown in Fig. 5(b) together with the middle curve of Fig. 5(a).

The effect that different range and strength of the spatial coupling have on the motion of interfaces in the bistable regime is shown in Fig. 6. In all examples the local dynamics is identical; the range of the coupling $\tilde{w}/L$ increases from left to right within one row, and the strength of the coupling $\tilde{\sigma}$ increases from top to bottom within one column. It can be seen clearly that it is the range that determines the qualitative behavior of the transition, i.e., whether the fronts move with constant velocity or whether they are accelerated. Its influence on the width of the interface is comparatively small, and the average velocity, though of course being larger in the case of the accelerated fronts, is not changed significantly. In contrast, and not surprisingly, the strength of the coupling has a pronounced effect on the width of the interface as well as on the velocity of the fronts, the latter also being found experimentally [28,30,44,45].

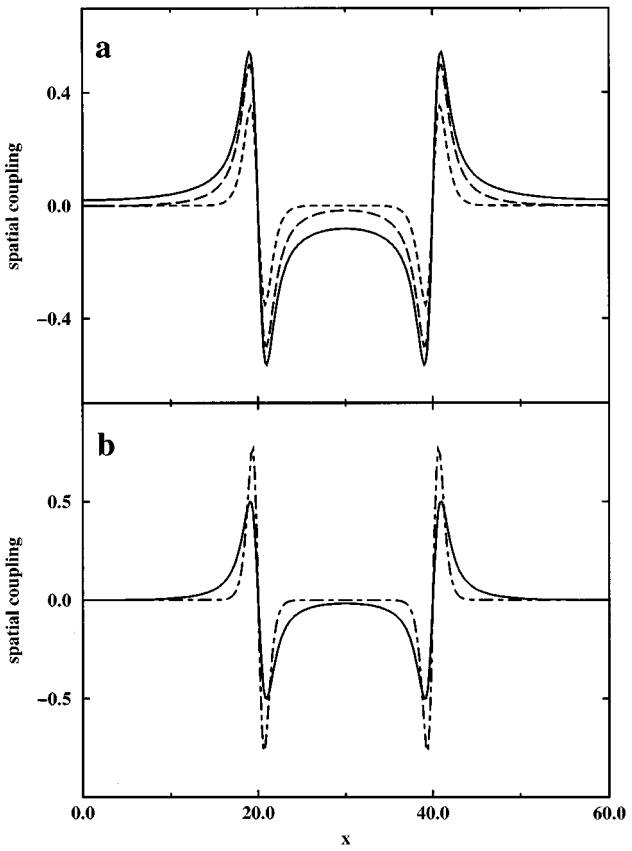

FIG. 5. (a) Spatial coupling term in Eqs. (8b) and (8c) for three values of w/L. (solid curve: $2\pi w/L=4$; long-dashed curve: $2\pi w/L=0.5$; dashed curve: $2\pi w/L=0.1$). (b) Comparison of the spatial coupling in an electrochemical system (solid line: $2\pi w/L=0.5$) and diffusive coupling (dashed line). The potential distribution at the electrode was chosen rectangular (similar to the one shown in Fig. 3) in both cases.

DISCUSSION

In the previous section it was shown that the range of the coupling in an electrochemical system depends crucially on the ratio of the two length scales which come into play in every electrochemical experiment: the size of the electrode L and the distance between working and reference electrode w. In order to understand in which range the coupling function can be tuned by changing w/L, it is instructive to investigate the limits of very short and very large distances between working and reference electrode.

For small w/L the spatial coupling is short range [Fig. 3(c)], and the simulations show that fronts move with constant velocity [Figs. 4(a) and 6, first column] which is in accordance with the behavior of reaction diffusion systems, and we call this limit the diffusive limit. This view can be substantiated if we consider the limit $w/L \to 0$, a case in which the coth term in Eqs. (8b) and (8c) can be expanded leading to the following expression for the coupling term:

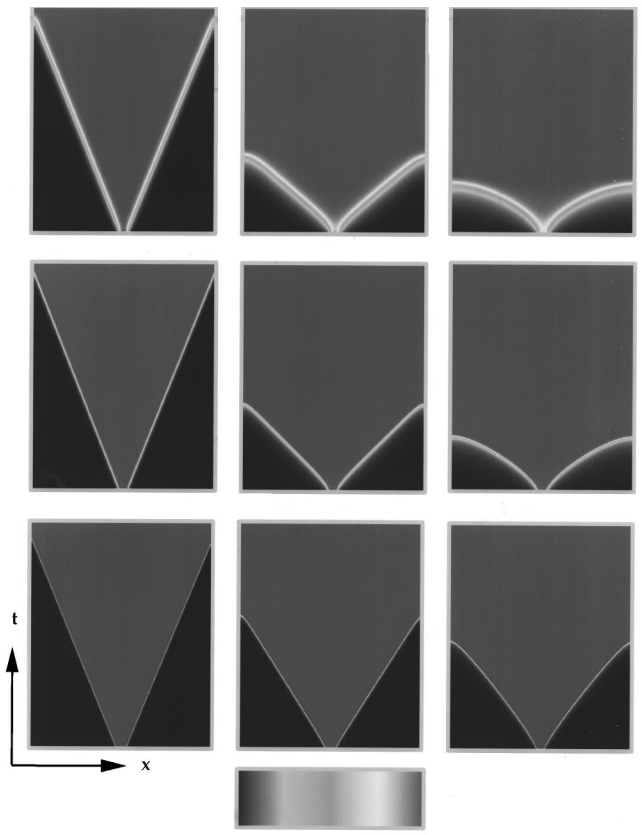

FIG. 6. Gray scale representation of the spatiotemporal evolution of the potential at $z=-1$ for different values of $\tilde{w}$ and $\tilde{\sigma}$. Top row: $\tilde{\sigma}=0.565$; middle row: $\tilde{\sigma}=0.0565$; and bottom row: $\tilde{\sigma}=0.00565$. Left column: $\tilde{w}=0.003$; middle column: $\tilde{w}=0.03$; and right column: $\tilde{w}=0.3$. (The remaining parameters are $V=-350$, $w=0.03$, $\sigma=1.596$ and $L=0.188$). The gray scale given at the bottom was chosen nonmonotonically for clarity.

$$\lim_{w/L\to 0}\left[-\sigma\, 2\pi n\, \coth\left(\frac{w}{L}\,2\pi n\right)\right] \approx -\frac{\sigma L}{w}-\frac{(2\pi)^2}{3}\,\frac{\sigma w}{L}\,n^2+\frac{(2\pi)^4}{45}\,\frac{\sigma w^3}{L^3}\,n^4 -\frac{2(2\pi)^6}{945}\,\frac{\sigma w^5}{L^5}\,n^6+O(n^8) \tag{11}$$

(This expansion is valid for arguments $<\pi$.) The first term in the series can be identified as the electrolyte contribution to the local dynamics. The remaining terms formally represent contributions of second, fourth, sixth, etc. spatial derivatives to the rate equations of the mode coefficients. Hence the second term can be considered as originating from a diffusional process. For $w/L\to 0$ the higher-order terms [being proportional to $(w/L)^{i-1}n^i$] can be neglected, and hence the coupling can be described by a diffusional process with diffusion constant $D=4\pi^2\sigma w/(3L)$. Note that in this case the apparent diffusion constant is proportional to w/L. The dependence of D on w tells us that although the coupling is strictly local in the direction parallel to the electrode, it is global in the direction perpendicular to it. This dependence also implies that for $w=0$ the spatial coupling vanishes as the diffusion constant becomes zero.

Now consider the limit $w/L\to\infty$, which we realize by setting the equipotential line at w to infinity. From Eq. (9) it is apparent that the contribution of the electrolyte to the local dynamics disappears, and as $\coth[(w/L)2\pi n]$ approaches 1 asymptotically for large arguments, the contribution of the coupling to the dynamics of the individual mode coefficients is proportional to n, with the proportional constant $2\pi\sigma$:

$$\lim_{w/L\to\infty}\left[-\sigma\, 2\pi n\, \coth\left(\frac{w}{L}\,2\pi n\right)\right]\approx -\sigma\, 2\pi n. \tag{12}$$

In this case the range of the coupling is maximum, and it becomes apparent that global coupling (in a sense that the coupling affects all space locations equally) cannot be realized by changing w/L, where the coupling would depend only on the homogenous mode ($n=0$). The right hand side of Eq. (12) is already a good approximation from $w/L\sim 0.5$ on, which means that in typical electrochemical experiments the coupling range is nearly maximum.

At this point it is important to emphasize again the difference between the effects that increasing the strength and increasing the range have on the dynamics. Increasing the strength of the coupling changes the ratio of the rates of reaction and diffusion. Hence the faster the diffusion, or, more generally, the faster the spatial communication compared to the reaction rate, the larger the diffusion length on the time scale of the reaction. It is well known that this leads to increasingly broader interfaces [1,2] and two fronts (e.g., emerging from a nucleus of one state within the other state as in Figs. 4 and 6) will eventually interact attractively. This also leads to an apparent acceleration in the spatiotemporal picture. Upon a further increase in the coupling strength, transitions in the bistable regime occur nearly homogeneously, and from this point of view the system can be considered to be globally coupled. This is, e.g., the case in Fig. 4(d). On the other hand, when altering the range of the coupling, the relative rates between reaction and spatial coupling stay constant, and the transition between constant and increasing velocity of fronts occurs at the same width of the interface. In this case the acceleration cannot be traced back to front interaction, but is due to the form of the coupling function. From these considerations it is also clear that long-range coupling can best be studied if the reaction rate is fast, compared to the rate of spatial communication, or in other words, if the strength of the coupling is weak (see the last row in Fig. 6).

Koper and Sluyters derived a model for pattern formation in electrochemical systems on the assumption that the potential distribution inside the electrolyte can be described by a linear z dependence up to a diffusion layer δ (typically on the order of 10–100 μm), beyond which it is homogeneous. From a physical point of view, this ansatz has to be criticized because it is well known that potential inhomogeneities reach far into the electrolyte and are still measurable in some mm distance [46]. Despite this, it is interesting to note that the ansatz leads to a reaction-diffusion system with a diffusion constant proportional to δ, or, if one extends the linear dependence up to the equipotential line, proportional to w. Consequently for small w/L this reaction-diffusion model is adequate, and merges with the model used here. For larger distances between working and reference electrode the

model fails to capture the long-range coupling and, in addition, overestimates the strength of the coupling (if the linear dependence is assumed up to w).

CONCLUSION

Electrochemical systems provide an easy experimental access to study the impact of the coupling range on pattern formation: the range of the coupling can be tuned by simply changing the geometry of the system, especially by adjusting the distance between working and reference (or counter) electrode. The coupling strength can be adapted by varying the conductivity of the solution. In the bistable regime an increase of the coupling range leads from constantly moving to accelerated fronts. The results presented here form a basis for the further study of effects of long-range coupling on different dynamic regimes, as, e.g., excitable or oscillatory dynamics. Furthermore, the model presented should be readily transferable to electrical continuum devices consisting of materials with nonlinear and linear characteristics, for example, those discussed in [47].

[1] A. S. Mikhailov, *Foundations of Synergetics I* (Springer, Berlin, 1994).
[2] J. D. Murray, *Mathematical Biology* (Springer, Berlin, 1990).
[3] M. Eiswirth, P. Möller, K. Wetzl, R. Imbihl, and G. Ertl, J. Chem. Phys. **90**, 510 (1989).
[4] S. Jakubith, H. H. Rotermund, W. Engel, A. von Oertzen, and G. Ertl, Phys. Rev. Lett. **65**, 3013 (1990).
[5] M. Falcke and H. Engel, Phys. Rev. E **50**, 1353 (1994).
[6] K. C. Rose, D. Battogtokh, A. Mikhailov, R. Imbihl, W. Engel, and A. M. Bradshaw, Phys. Rev. Lett. **76**, 3582 (1996).
[7] M. A. Liauw, P. J. Plath, and N. I. Jaeger, J. Chem. Phys. **1044**, 6375 (1996).
[8] E. Schöll, *Nonequilibrium Phase Transitions in Semiconductors* (Springer, Berlin, 1987).
[9] R. P. Huebener, Adv. Solid State Phys. **30**, 387 (1990).
[10] J. Peinke, W. Clauss, R. P. Huebener, A. Kittel, J. Parisi, U. Rau, and R. Richter, in *Spontaneous Formation of Space-time Structures and Criticality*, edited by T. Riste and D. Sherrington (Kluwer, Dordrecht, 1991).
[11] H. Willebrand, F.-J. Niedernostheide, E. Ammelt, R. Dohmen, and H.-G. Purwins, Phys. Lett. A **153**, 437 (1991).
[12] H. Willebrand, T. Hünteler, F.-J. Neidernostheide, R. Dohmen, and H.-G. Purwins, Phys. Rev. A **45**, 8766 (1992).
[13] E. Ammelt, D. Schweng, and H.-G. Purwins, Phys. Lett. A **179**, 348 (1993).
[14] S. Grill, V. S. Zykov, and S. C. Müller, Phys. Rev. Lett. **75**, 3368 (1995).
[15] U. Middya and D. Luss, J. Chem. Phys. **100**, 3568 (1994).
[16] F. Mertens, R. Imbihl, and A. Mikhailov J. Chem. Phys. **101**, 9903 (1994).
[17] D. Battogtokh, A. Preusser, and A. Mikhailov (unpublished).
[18] I. Schebesch and H. Engel, in: *Self-Organization in Activator-Inhibitor Systems: Semiconductors, Gas Discharge and Chemical Active Media*, edited by H. Engel, F.-J. Niedernostheide, H. G. Purwins, and E. Schöll (Wissenschaft und Technik, Berlin, 1996).
[19] K. Krischer and A. Mikhailov, Phys. Rev. Lett. **73**, 3165 (1994).
[20] Th. Christen, Z. Naturforsch. **50a**, 1128 (1995).
[21] F.-J. Niedernostheide, M. Ardes, M. Or-Guil, and H.-G. Purwins, Phys. Rev. B **49**, 7370 (1994).
[22] M. Or-Guil, E. Ammelt, F.-J. Niedernostheide, and H.-G. Purwins, in *Nonlinear Dynamics and Pattern Formation in the Natural Environment*, edited by A. Doelman and A.v. Harten, Pitman Research Notes in Mathematics Series Vol. 335 (Longman, London, 1995).
[23] L. Schimansky-Geier, Ch. Zülicke, and E. Schöll, Physica A **188**, 436 (1992).
[24] F. J. Elmer, Physica D **30**, 321 (1988).
[25] Y. Kuramoto and H. Nakao, Phys. Rev. Lett. **76**, 4352 (1996).
[26] Y. Kuramoto (unpublished).
[27] Y. Kuramoto and H. Nakao (unpublished).
[28] G. Flätgen and K. Krischer, Phys. Rev. E **51**, 3997 (1995).
[29] G. Flätgen and K. Krischer, J. Chem. Phys. **103**, 5428 (1995).
[30] G. Flätgen, K. Krischer, and G. Ertl, Z. Naturforsch. **50a**, 1097 (1995).
[31] R. D. Otterstedt, N. I. Jaeger, and P. J. Plath, Int. J. Bifurcation Chaos **4**, 1265 (1994).
[32] R. D. Otterstedt, P. J. Plath, N. I. Jaeger, and J. L. Hudson, Phys. Rev. A **54**, 3744 (1996).
[33] G. Flätgen, Ph.D. thesis, Freie Universität, 1995 (unpublished).
[34] M. T. M. Koper and J. H. Sluyters, Electrochim. Acta **38**, 1535 (1993).
[35] A. Wacker and E. Schöll, J. Appl. Phys. **78**, 7352 (1995).
[36] H. Degn, Trans. Faraday Soc. **64**, 1348 (1968).
[37] M. T. M. Koper, Electrochim. Acta **37**, 1771 (1992).
[38] W. Wolf, J. Ye, M. Purgand, M. Eiswirth, and K. Doblhofer, Ber. Bunsenges. Phys. Chem. **96**, 1797 (1992).
[39] M. T. M. Koper, in *Advances in Chemical Physics XCII*, edited by I. Prigogine and S. A. Rice (Wiley, New York, 1996).
[40] A. J. Bard and L. R. Faulkner, *Electrochemical Methods* (Wiley, New York, 1980).
[41] A. C. Hindmarsh, ACM-SIGNUM Newsl. **15**, 10 (1980). lsode is available from the netlib library.
[42] C. Canuto, A. Quarteroni, M. Hussaini, and T. A. Zang, *Spectral Methods in Fluid Dynamics* (Springer, Berlin, 1988).
[43] Note that we use the term front throughout the paper somewhat loosely for interfaces between the two steady states in the bistable regime. In a more rigorous sense, a front is a traveling-wave solution. In a bistable regime the latter can only exist in infinitely extended systems.
[44] K. F. Bonhoeffer and W. Renneberg, Z. Phys. **118**, 389 (1941).
[45] U. F. Franck, Z. Elektrochem. **55**, 154 (1951).
[46] H. S. Isaacs and G. Kissel, J. Electrochem. Soc. **119**, 1628 (1972).
[47] H. G. Purwins, C. Radehaus, T. Dirksmeyer, R. Dohmen, R. Schmeling, and H. Willebrand, Phys. Lett. A **136**, 480 (1989).